Fragment recognition in molecular dynamics

A. Strachan and C. O. Dorso
Departamento de Fisica, Facultad de Ciencias Exactas y Naturales, Universidad de Buenos Aires, Pabellón I, Ciudad Universitaria, Nuñez (1428), Buenos Aires, Argentina
(Received 22 October 1996)

We investigate the properties of three methods of fragment recognition in microscopic simulations of molecular dynamics. They are (a) the early cluster recognition algorithm (ECRA) which looks for the most bound partitions in phase space, (b) the minimum spanning tree in two particle energy space (MSTE) which looks for those simply connected partitions in which each particle is bound to, at least, one other member of the cluster to which it belongs, and (c) the standard minimum spanning tree (MST) in configuration space. It is found that, if the objective of a given calculation is to study the time evolution of properties related to the fragment distribution, the MST should be discarded, MSTE results will be valid for not too short times, and ECRA results will give the most complete description of such properties. [S0556-2813(97)01308-3]

PACS number(s): 25.70.Pq, 02.70.Ns, 24.10.Lx

I. INTRODUCTION

The problem of fragmentation of finite excited systems is a topic of current interest in many branches of physics, encompassing phenomena involving very different scales and interaction potentials which range from nuclear multifragmentation to the explosion of hot and dense liquid drops. The possibility of finding power-law fragment distributions, i.e., scale-free mass spectra, in such different systems opens the possibility of facing universality class in fragmenting systems [1].

The study of these kind of processes has strongly benefited from classical microscopic simulations, which give us the possibility of dealing with the complete microscopic information in $(\mathbf{q},\mathbf{p})$ space, thus allowing us to study correlations of all orders. On the other hand, handling such an enormous amount of information is not an easy task; the determination of the fragment production process has been particularly elusive.

Heavy-ion collisions at intermediate energy are a proper tool to learn about the nuclear equation of state. It is then mandatory to understand the information contained in the asymptotic mass spectrum and to which state of the evolution of the fragmenting system it refers. For this sake, it is important to properly analyze the time evolution of fragment formation and to understand which kind of information is provided by the fragment recognition algorithm being used. It is the purpose of this work to study and compare the fragment recognition algorithms which are currently used.

In this paper we compare the results obtained from the analysis of the numerical simulations of excited two-dimensional disks build up of $N=100$ particles and excited three-dimensional spheres of $N=147$ particles interacting via a Lennard-Jones potential which undergo fragmentation and display, asymptotically, power-law mass spectra.

In Sec. II we define the fragment recognition algorithms and the model used to simulate the fragmentation of two-dimensional disks and three-dimensional drops. In Sec. III we present the results of applying the above mentioned fragment recognition algorithms to the microscopic simulations performed and the comparison and analysis of the different outputs. Finally conclusions are drawn.

II. MODEL AND FRAGMENT RECOGNITION ALGORITHMS

The most widely used algorithm for recognizing fragments is the standard minimum spanning tree (MST) in configuration space which has been borrowed from simpler problems such as percolation theory. In this approach a cluster is defined in the following way. Given a set of particles $i,j,k,\ldots$, they belong to a cluster C if

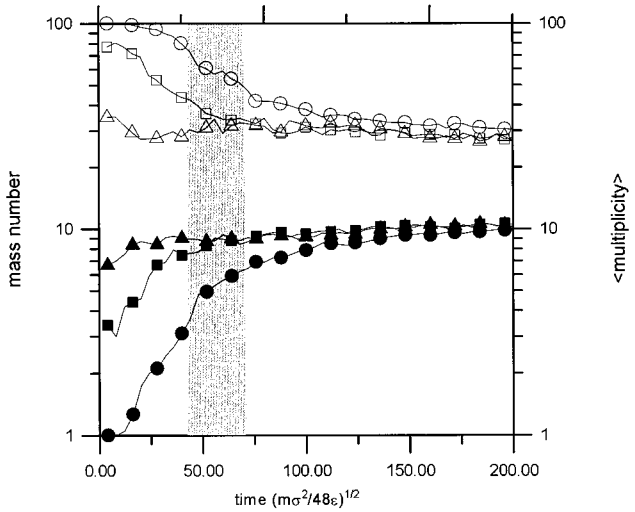

FIG. 1. In this figure we show the time evolution of the size of the biggest fragment (empty symbols) and of the multiplicity for fragments bigger than 3 (full symbols) for an initial energy of $E=-0.55\epsilon$. In this figure results are shown for the three fragment recognition algorithms described in the main text. It is immediately seen that the simple MST approach (circles) is unable to properly analyze the configurations that are not very close to the asymptotic stage of the evolution. MSTE (squares) results give the asymptotic results earlier than MST, and ECRA (triangles) is the one that shows that fragments are already formed even earlier in the very dense stage of the evolution.

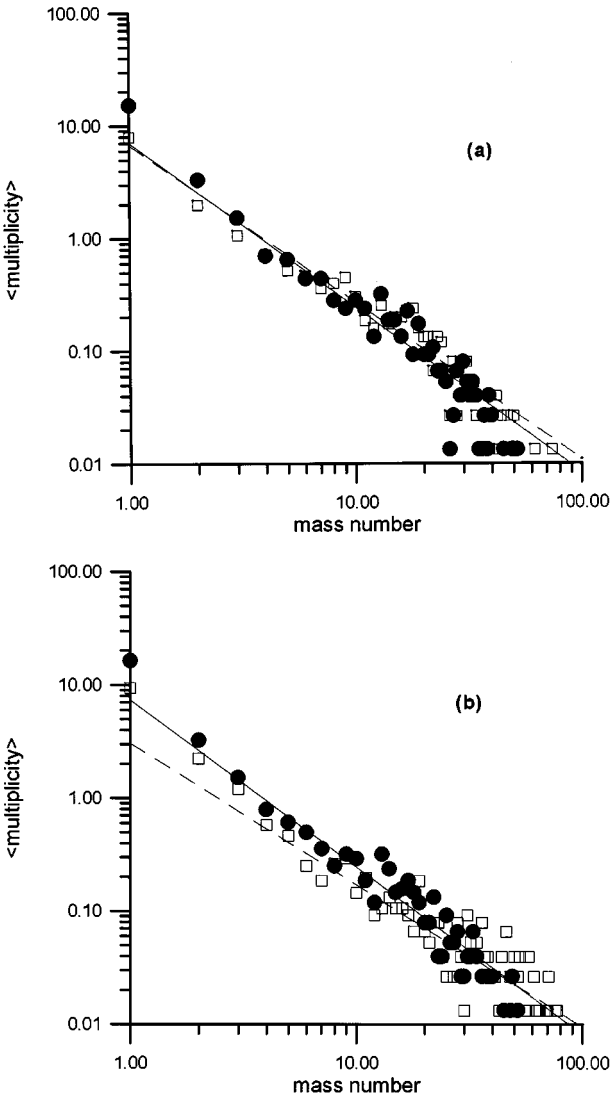

FIG. 2. In this figure we show the mass spectrum for $N=100$ particles LJ disks with an initial energy of -0.55ϵ at $t=200t_0$ (full circles) and $t=40t_0$ (empty squares) according to the ECRA analysis (a) and the MSTE analysis (b) together with the corresponding power-law fits. The fits at $t=200t_0$ are denoted by full line and the ones for $t=40t_0$ by dashed lines.

$$\nabla i \in C, \exists j \in C / |\mathbf{r}_i - \mathbf{r}_j| \leqslant R_{\mathrm{cl}}, \tag{1}$$

where $\mathbf{r}_i$ and $\mathbf{r}_j$ denote the positions of the particles and R_{cl} is a parameter usually referred to as the clusterization radius. This is an arbitrary parameter fixed according to taste. Usually the interparticle potentials used in microscopic simulations are truncated at a cutoff distance R_{co}. So the following relation must hold: $R_{\mathrm{cl}} \leqslant R_{\mathrm{co}}$. In this cluster definition the role of relative momentum of particles is totally disregarded. We will denote this kind of approach as MST. It should be clear from the definition that this method can only be used to analyze asymptotic configurations in which the fragmenting system can be viewed as a very dilute mixture of free particles and almost equilibrated fragments, nevertheless it is used in the dense stage of the evolution giving, consequently, wrong results (see, for example, [2,3]).

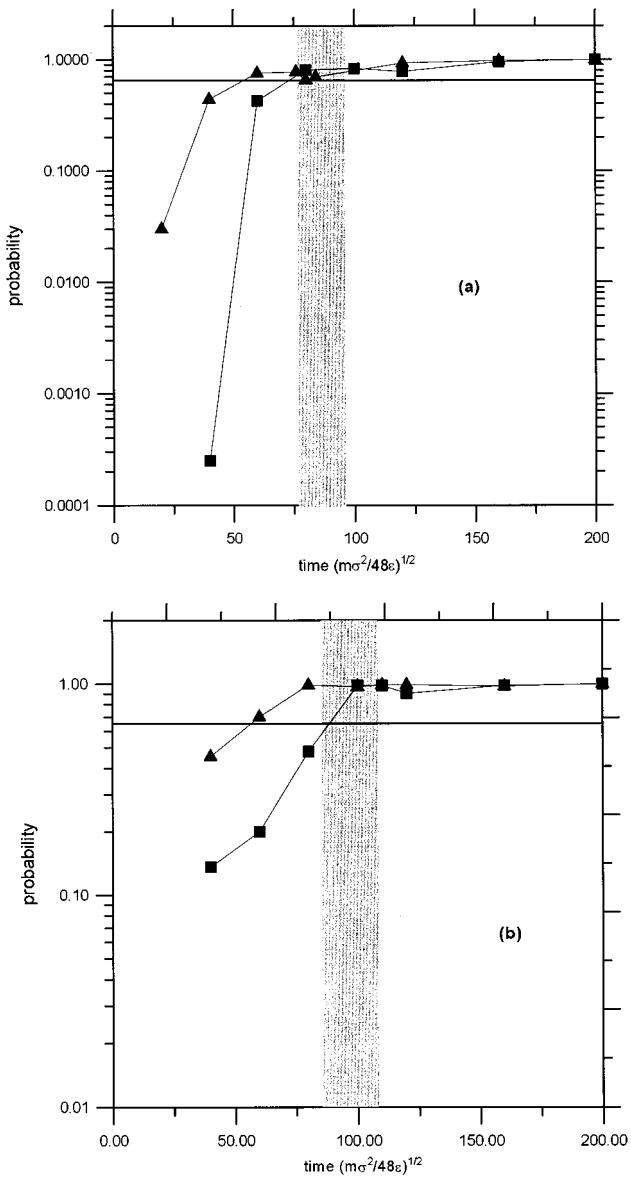

FIG. 3. In this figure we show the time dependence of the probability that the spectra at time t is statistically equivalent to the asymptotic one according to the χ^2 test for binned data. (a) Corresponds to energy $E=-0.55\epsilon$ and (b) for $E=-0.8\epsilon$. In both cases triangles denote ECRA results and squares stand for the MSTE results. It is immediately seen that statistical stability is reached by ECRA at earlier times. Shaded region denotes the time range for equivalence between both analysis.

An improvement over the MST algorithm, although in the same spirit, is to look for simply connected structures in the space of two-particle binding energy [4,5]. This model, which we denote as MSTE, is defined in the following way. As before i,j denote particles and C stands for a cluster; then a cluster is a set of particles such that

$$\nabla i \in C, \exists j \in C / e_{ij} \leqslant 0, \tag{2}$$

with $e_{ij} = V_{ij} + (\mathbf{p}_i - \mathbf{p}_j)^2/4\mu$, where μ is the reduced mass. So the cluster is built out of bound pairs of particles. It is clear that in this case the effects of momentum are, in some way, taken into account.

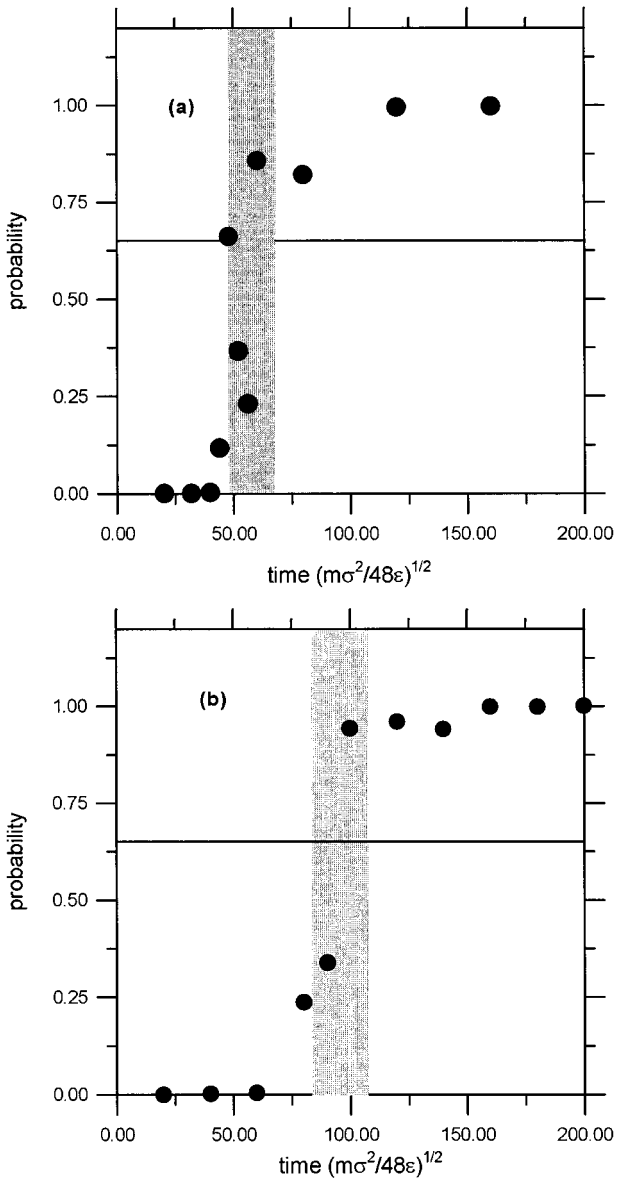

FIG. 4. In this figure we show the probability that at each time step the mass spectra provided by ECRA and MSTE analysis are statistically equivalent. In (a) $E=-0.55\epsilon$ and in (b) $E=-0.8\epsilon$; once again the shaded region denotes the time range for equivalence between both analysis.

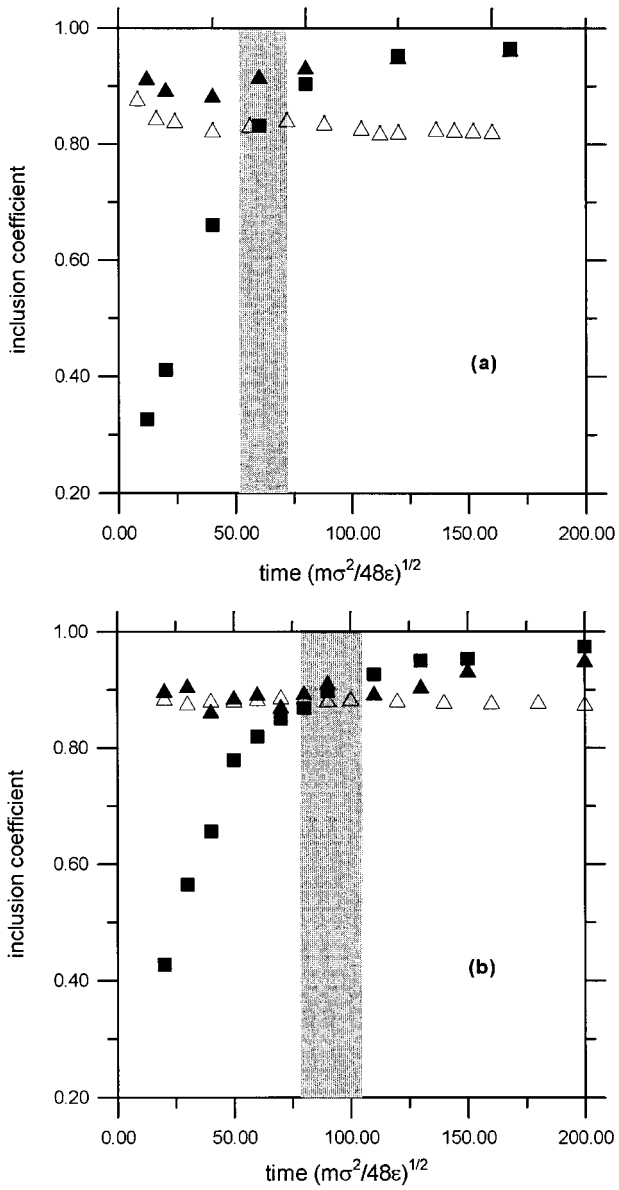

FIG. 5. In this figure we show the inclusion coefficient $I(t)$ as a function of time for $E=-0.55\epsilon$ (a) and $E=-0.8\epsilon$ (b). ECRA on MSTE is denoted by full triangles, MSTE on ECRA by squares; empty triangles refer to the reference value (see text for details).

Finally we briefly describe the third method which we dubbed the early cluster recognition algorithm (ECRA) [6], in which clusters are defined as the most bound partition of the system, i.e., the partition (defined by the set of clusters $\{C_i\}$) that minimizes the sum of the energies of each fragment:

$$E_{\{C_i\}}=\sum_i \left[\sum_{j\in C_i} K_j^{\text{c.m.}}+\sum_{j,k\in C_i} V_{j,k}\right], \tag{3}$$

where the first sum is over the clusters of the partition and $K_j^{\text{c.m.}}$ is the kinetic energy of particle j measured in the center-of-mass frame of the cluster which contains particle j. The algorithm developed to achieve this goal is based on an optimization method in the spirit of simulated annealing [6], and therefore poses strong demands on computer time. The partition obtained using this last approach will be called hereafter the most bound density fluctuation. We will denote its constituent clusters as fragments only in the low-density regime, i.e., when they coincide with the MST fragments.

As mentioned in the Introduction we simulate multifragmentation via a classical system of Lennard-Jones particles in two dimensions. The two-body interaction potential is taken as

$$V(r)=4\epsilon\left[\left(\frac{\sigma}{r}\right)^{12}-\left(\frac{\sigma}{r}\right)^{6}-\left(\frac{\sigma}{r_c}\right)^{12}+\left(\frac{\sigma}{r_c}\right)^{6}\right], \tag{4}$$

where r_c is the cutoff radius (the potential is taken equal to zero for $r>r_c$). In these calculations we took $r_c=3\sigma$. Energy and distance are measured in units of the potential well

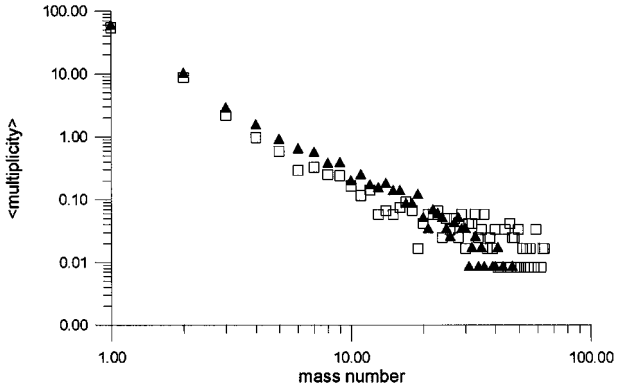

FIG. 6. Asymptotic mass spectra of the three-dimensional drops for enegies $E=0.5\epsilon$ (squares) and $E=1.2\epsilon$ (triangles).

(ϵ) and the distance in which the potential changes sign (σ), respectively. The unit of time that we used is $t_0=\sqrt{\sigma^2 m/48\epsilon}$.

In this work we study numerical simulations of the time evolution of excited, two-dimensional Lennard-Jones (LJ) drops of $N=100$ particles, whose initial configurations were obtained by cutting a circular drop from a thermalized periodic system of $N=225$ LJ particles, per cell, with periodic boundary conditions. The ground-state energy ϵ_0 of this system of 100 LJ particles, was calculated from an almost circular system cut out from a triangular lattice; the distance between nearest neighbors was taken as that distance at which $V(r)$ attains its minimum value ($r_{\min}\sim 1.12\sigma$). We obtained $\epsilon_0\simeq -2.8\epsilon$. An analysis for a rather broad range of energies was performed in Ref. [7] (hereafter referred to as I). In this work we will focus on energies of $E=-0.8\epsilon$ and -0.55ϵ, because these are the cases in which the asymptotic mass spectra turn out to, approximately, show power-law behavior. The initial density is in all the cases $\rho=0.75\sigma^{-2}$. This means that all our drops are compressed and heated. See I for details. For the three-dimensional case the methodology is the same. Spherical drops are cut from a thermalized 3D periodic system of $N=512$ particles per cell. Three different energies are analyzed in this work, namely, $E=1.2\epsilon$, $E=0.9\epsilon$, and $E=0.5\epsilon$, the initial density is always $\rho=0.85\sigma^{-3}$.

III. ANALYSIS OF NUMERICAL EXPERIMENTS

In what follows we analyze the configurations resulting from the microscopic simulation of the time evolution of highly excited two-dimensional disks and three-dimensional spheres. We begin with the two-dimensional case and afterwards we extend the analysis to the three-dimensional one.

We first focus on the time evolution of the mean multiplicity for fragments bigger than 3 and the time evolution of the mean size of the largest fragment according to MST, MSTE, and ECRA, for the two-dimensional case. In Fig. 1 we show these quantities for energy $E=-0.55\epsilon$, see caption for details. It is immediately seen that the MST completely fails to analyze the initial stages of the evolution. On the other hand, it can be seen that ECRA results attain their asymptotic values at very early times. As regards MSTE, it approaches the ECRA result at rather early times. Taking into account that it is obvious that MST is quite unreliable

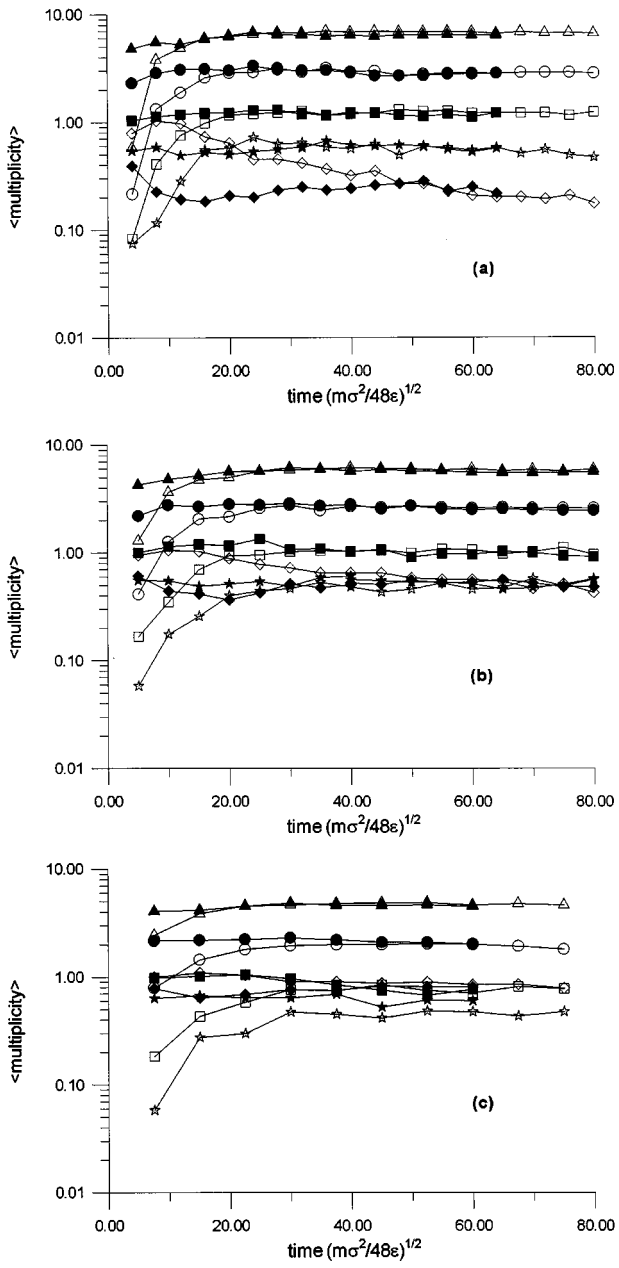

FIG. 7. Mean multiplicity as a function of time for different mass ranges: 3–7 (triangles), 5–9 (circles), 10–15 (squares), 20–30 (stars), and bigger than 30 (diamonds). The shaded symbols denote ECRA results and empty symbols MSTE results. The energies are $E=1.2\epsilon$ (a), $E=0.9\epsilon$ (b), and $E=0.5\epsilon$ (c).

for early stages of the evolution, from now on we focus on MSTE and ECRA only. It is worth mentioning at this point that we consider the system to be in its asymptotic state, as regards to fragment formation, when the results obtained by the three methods coincide.

In Fig. 2(a) we show the asymptotic mass spectrum for $E=-0.55\epsilon$, at time $t=200t_0$ (full circles) according to the ECRA formalism and the result of a power-law fit (full line); we also show the mass spectrum for time $t=40t_0$ according to ECRA (squares) and its corresponding power-law fit (dashed line). The mass number fit range used was $4\leqslant A\leqslant 34$. We obtained the exponent $\tau=1.46$ for $t=200t_0$ and $\tau=1.39$ for $t=40t_0$. In Fig. 2(b) we show the mass

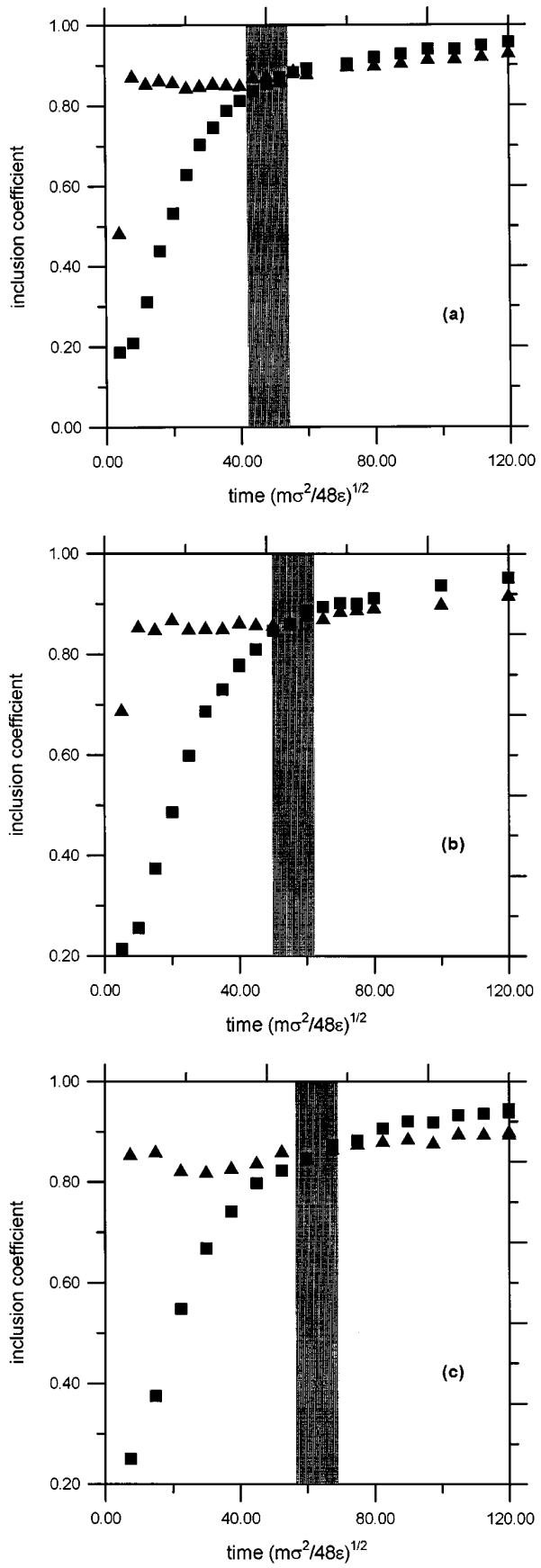

FIG. 8. Inclusion coefficient for the three-dimensional case as a function of time. ECRAS on MSTE is denoted by triangles and MSTE on ECRA by squares. The energies are $E=1.2\epsilon$ (a), $E=0.9\epsilon$ (b), and $E=0.5\epsilon$ (c).

spectrum at time $t=200t_0$ (full circles) and $t=40t_0$ but according to the MSTE algorithm and their corresponding power-law fits. The exponents found are $\tau=1.47$ for $t=200t_0$ and $\tau=1.25$ for $t=40t_0$. It is clear that asymptotically both algorithms give the same result, and that ECRA result at time $t=40t_0$ is very similar to the asymptotic one, while at this time the MSTE method gives little information about the final behavior.

The next step should be to compare the mass spectra resulting from these two algorithms and their statistical properties. A natural comparison concerns the moments of the resulting distributions as a function of time. Instead of this we choose a more direct way. We ask ourselves at which stage of the evolution the statistical properties of the distributions resulting from MSTE and ECRA are compatible with the asymptotic one. For this purpose we use the chi square statistics for binned data (χ_b^2) [7] defined by

$$\chi_b^2=\sum_i \frac{(b_i-a_i)^2}{(b_i+a_i)}, \tag{5}$$

where b_i denotes the population of bin i for data set $\{b\}$ and a_i the corresponding for data set $\{a\}$. From this quantity we can calculate the probability that the two sets $\{a\}$ and $\{b\}$ come from the same probability density distribution function [8]. Taking into account that we are interested in comparing the ECRA and MSTE spectra as a function of time with the asymptotic spectrum, we fix data set $\{a\}$ as corresponding to the final mass spectrum and calculate χ_b^2 using for $\{b\}=\{b(t)\}_{\mathrm{ECRA}}$ and $\{b\}=\{b(t)\}_{\mathrm{MSTE}}$. Rather than considering the complete spectrum we focus on the range of intermediate mass fragments $4\leqslant A\leqslant 34$, due to the fact that the lighter mass bins are constantly populated by evaporation in heavier fragments. On the other hand, for energies that give rise to power-law mass spectra the heavier fragments are expected to have very large fluctuations from event to event due to critical phenomena behavior [9] and to finite-size effects. To estimate the value of the probability of the χ_b^2 test denoting equivalence we have studied this magnitude when different mass spectra are generated from the same probability density distribution function. For this purpose we have generated sets of 100 partitions with total mass $N=100$ from a power-law distribution, as is done in the Elattari-Richert-Wagner model of fragmentation [10]. After calculating χ_b^2 and averaging we obtained a limit of confidence of 65%. In Fig. 3(a) we show the results of the corresponding probabilities for energy $E=-0.55\epsilon$ and in Fig. 3(b) for $E=-0.8\epsilon$. It is clearly seen that ECRA results for $E=-0.55\epsilon$ attain statistical stability at time $\sim 50t_0$ which is shorter than that for the MSTE results ($\sim 80t_0$); for $E=-0.8\epsilon$ the picture is exactly the same but the times are a little longer: ~ 60 for the stability of the ECRA spectrum and $\sim 90t_0$ for MSTE. The shaded regions in Figs. 3(a) and 3(b) denote the time at which the MSTE result becomes statistically equivalent to the asymptotic one.

In Fig. 4(a) we show the probability that the ECRA spectra and the MSTE spectra at a given time, come from the same density distribution function for $E=-0.55\epsilon$, and in Fig. 4(b) we show the same quantity but for $E=-0.8\epsilon$; the shaded regions denote the time at which both kind of analy-

sis become equivalent. Comparing Figs. 3 and 4 it is seen that both the ECRA and MSTE results come from the same distribution with high probability by the time that both spectra are consistent to a high degree with the asymptotic one.

In order to further explore the relation between both results we compare the microscopic consistency between the composition of the fragments detected by each recognition algorithm event by event as a function of time. For this purpose we use the coefficient of inclusion at time t, $I(t)$ defined by the following argument. Let $n_1, n_2 \cdots n_N$ be the nucleons belonging to a given ECRA cluster C_E^j with mass number $A_{C_j} = n_N$ at time t; $b_j(t) = 0.5 * n_N(n_N - 1)$ is then the number of pairs of nucleons in cluster C_E^j at that time. The mass spectrum according to ECRA is then $\{C_E^j\}$. At the same time, for the same microscopic configuration we will have a set of clusters $\{C_M^i\}$, according to MSTE. They may differ in its microscopic structure which means that particles that are together in some C_E^i may be scattered among two or more elements of $\{C_M^i\}$. Let $N_{C_E^j \to C_M^i}$ be the number of nucleons which belong to cluster C_E^j and also belong at time t to a C_M^i. The number of pairs of nucleons which belong to ECRA cluster j at time t and also belong to a given MSTE cluster at that time is then $a_j(t) = \Sigma_i 0.5 * [N_{C_E^j \to C_M^i}(N_{C_E^j \to C_M^i} - 1)]$, where the sum runs over all clusters according to the MSTE algorithm. We are now able to introduce the mass weighted inclusion coefficient $[I_m(t)]$

$$I_{E \to M}(t) = \left\langle \left\langle \frac{a_j(t)}{b_j(t)} A_{Cj} \right\rangle_{\rm cl} \right\rangle_e \tag{6}$$

where $\langle\ \rangle_{\rm cl}$ denotes average over the clusters at time t and $\langle\ \rangle_e$ denotes average over the ensemble of explosions at a given energy. $I_{E \to M}(t)$ will be equal to 1 if all pairs of particles in a given cluster according to ECRA belong to the same cluster when the system is studied with the MSTE approach. It is worth mentioning at this point that this does not mean that both algorithms give exactly the same result but that the ECRA algorithm breaks up the MSTE clusters. On the other hand, the inclusion coefficient would be 0 if the arrangement were completely different. It measures the tendency of the members of a given cluster recognized by ECRA to be together in the MSTE analysis. Equivalently one can define $I_{M \to E}(t)$ which measures the tendency of constituents of fragments recognized by MSTE to be together in ECRA.

In Figs. 5(a) and 5(b) we show the coefficient $I_{E \to M}(t)$ (full triangles) together with $I_{M \to E}(t)$ (squares) for the same energies as before, see caption for details. A third curve is drawn in which the value of $I_{E \to M'}(t)$ in which $\{C_{M'}^i\}$ is obtained from $\{C_E^j\}$ by simply removing one particle from each fragment recognized by ECRA (empty triangles). This is our limit of microscopic consistency. It is seen that, for both energies fragments by ECRA are almost completely included into MSTE from the very outset. On the other hand, clusters detected by MSTE become included into the ECRA ones only after the time of statistical equivalence. If we now compare the characteristic times resulting from the shaded areas in Figs. 3, 4, and 5 it is easily seen that the resulting times for the equivalence of the results from MSTE and ECRA are the same irrespective of which of the three criteria is used.

We now focus on the analysis of the time evolution of our three-dimensional drops. In Fig. 6 we show the asymptotic mass spectra for the two extremal energies above mentioned, i.e., $E = 1.2\epsilon$ and $E = 0.5\epsilon$. It is clearly seen that their functional dependency is of the power-law type. In Fig. 7 we display the time evolution of the population of different bins according to the MSTE and ECRA algorithms (see figure caption for details). The same behavior as in the two-dimensional case is clearly seen. Finally, following the analysis performed in the two-dimensional case, we show in Fig. 8 the coefficients $I_{E \to M}(t)$ and $I_{M \to E}(t)$. Once again the depicted behavior is similar as the one obtained for the two-dimensional numerical experiments

IV. CONCLUSIONS

The results depicted in the previous section show that an analysis of the early (relevant) stages of fragment formation can only be accomplished by the application of the ECRA algorithm. For longer times MSTE will give comparable results.

Once the properties of the two relevant methods considered in this calculation (MST was disregarded early in the paper) have been established, we ask ourselves which other property would play a role in the choice of either. The answer is computing time. ECRA is much more computer time consuming than MSTE. The best way of combining both algorithms is to use MSTE and calculate the time at which it reaches statistical stability, then use ECRA for earlier times. Finally never use MST unless you are interested in asymptotic properties only, and you are sure that your numerical simulations have reached that stage of the evolution.

It is clear then, that, for the time being, ECRA is the right tool to unveil the dynamics of fragment formation and to determine the true break-up time. The information carried by the asymptotic spectra correspond to the state of the system at this break-up time. The next goal to get a deeper understanding of the fragmentation process is to determine the break-up state from the information contained in the asymptotic fragments, i.e., experimental data. We are currently working on this problem and results will be published in the near future.

ACKNOWLEDGMENTS

The authors gratefully acknowledge E. S. Hernandez for carefully reading this manuscript. This work was done under partial financial support from Universidad de Buenos Aires via Grant No. EX-070. C.O.D is a member of the Carrera del Investigador Cientifico CONICET-ARGENTINA and A.S. acknowledges the Universidad de Buenos Aires for financial support.

[1] R. Botet and M. Ploszajczak, Int. J. Mod. Phys. E **3**, 1633 (1994).
[2] J. Aichelin, Phys. Rep. **5&6**, 233 (1991).
[3] V. Latora, M. Belkacem, and A. Bonasera, Phys. Rev. C **52**, 271 (1995).
[4] S. Pratt, C. Montoya, and F. Romming, Phys. Lett. B **349**, 261 (1995).
[5] J. Pan and S. Das Gupta, Phys. Rev. C **51**, 1384 (1995).
[6] C. O. Dorso and J. Randrup, Phys. Lett. B **301**, 328 (1993).
[7] A. Strachan and C. O. Dorso, Phys. Rev. C **55**, 1 (1997).
[8] W. H. Press, B. P. Flannery, S. A. Teukolsky, and W. T. Vetterling, *Numerical Recipes, The Art of Scientific Computing* (Cambridge University Press, Cambridge, England, 1986).
[9] X. Campi and H. Krivine, Nucl. Phys. **A589**, 505 (1995).
[10] B. Elattari, J. Richert, and P. Wagner, Phys. Rev. Lett. **69**, 45 (1992); Nucl. Phys. **A560**, 603 (1993).